MCB
Journals.ASM.org

An Enhanced H/ACA RNP Assembly Mechanism for Human Telomerase RNA

Emily D. Egan and Kathleen Collins

Department of Molecular and Cell Biology, University of California at Berkeley, Berkeley, California, USA

The integral telomerase RNA subunit templates the synthesis of telomeric repeats. The biological accumulation of human telomerase RNA (hTR) requires hTR H/ACA domain assembly with the same proteins that assemble on other human H/ACA RNAs. Despite this shared RNP composition, hTR accumulation is particularly sensitized to disruption by disease-linked H/ACA protein variants. We show that contrary to expectation, hTR-specific sequence requirements for biological accumulation do not act at an hTR-specific step of H/ACA RNP biogenesis; instead, they enhance hTR binding to the shared, chaperone-bound scaffold of H/ACA core proteins that mediates initial RNP assembly. We recapitulate physiological H/ACA RNP assembly with a preassembled NAF1/dyskerin/NOP10/NHP2 scaffold purified from cell extract and demonstrate that distributed sequence features of the hTR 3′ hairpin synergize to improve scaffold binding. Our findings reveal that the hTR H/ACA domain is distinguished from other human H/ACA RNAs not by a distinct set of RNA-protein interactions but by an increased efficiency of RNP assembly. Our findings suggest a unifying mechanism for human telomerase deficiencies associated with H/ACA protein variants.

Incomplete genome replication by DNA-templated DNA polymerases can lead to progressive shortening of the telomeric repeats that cap eukaryotic nuclear chromosomes (36). To maintain chromosome integrity, the RNP enzyme telomerase compensates for terminal sequence loss by new repeat synthesis, for example, adding tandem repeats of TTAGGG in human cells. At the catalytic core of human telomerase, a structured 451-nucleotide (nt) telomerase RNA (hTR) provides the template for repeat synthesis by telomerase reverse transcriptase (49). Numerous proteins must associate with hTR to direct the biological specificity of precursor synthesis, processing, and RNP assembly as well as to direct mature RNA trafficking, localization, and catalytic activation (4). Improved knowledge of human telomerase RNP biogenesis and regulation should provide new strategies for enzyme activation and inhibition as disease therapies (39).

Human and other vertebrate telomerase RNAs, but not ciliate or yeast telomerase RNAs, have a 3′ domain shared with the evolutionarily ancient H/ACA RNA family (7, 32). H/ACA RNAs generally function as guides for site-specific pseudouridylation of a target RNA. Eukaryotic H/ACA small nucleolar RNAs (snoRNAs) modify ribosomal RNAs, while small Cajal body RNAs (scaRNAs) modify small nuclear RNAs (20, 24). Eukaryotic H/ACA RNAs have a universally conserved 5′ hairpin-hinge (H box)-3′ hairpin-ACA structure, including unpaired pockets in the hairpin stems that hybridize to target RNA sequence flanking the substrate uridine. The hairpin pockets of vertebrate telomerase RNAs show little if any phylogenetic sequence conservation (37), and no complementary putative target RNA(s) has been identified. In contrast to this functional divergence, hTR and pseudouridylation guide RNAs share the cellular requirement for structural integrity of the H/ACA motif, including the H box (ANANNA) and ACA sequences, as a prerequisite for assembly of a biologically stable RNP. The 5′ hairpin of the hTR H/ACA motif deviates from the pseudouridylation guide RNA consensus in its atypical spacing of the apex of the 5′ hairpin pocket from the H box; but the H box and lower stem of the 5′ hairpin are nonetheless critical for hTR maturation and RNP accumulation *in vivo*, and the presence of a hairpin pocket is strongly stimulatory (13, 32, 33). Therefore, albeit with structural deviations, the hTR H/ACA domain shares the two-hairpin secondary structure common to all eukaryotic H/ACA RNAs.

Assays of protein recruitment to an ectopic site of H/ACA RNA synthesis suggest that four proteins become rapidly associated with the RNA transcript: dyskerin, NOP10, NHP2, and NAF1 (8). Cotranscriptional RNP assembly protects the H/ACA RNA sequence from alternative processing or exonucleolytic degradation (1, 38, 48). The RNP subunit with pseudouridylase activity, termed dyskerin in human cells (also NAP57 or Cbf5p), binds to NOP10, which in turn binds to NHP2 to constitute the core heterotrimer (20, 24). Dyskerin also binds the H/ACA RNP assembly chaperone NAF1 (14), which is exchanged after initial RNP assembly for the fourth mature RNP protein, GAR1 (8). Reticulocyte lysate-expressed core heterotrimer proteins alone, with or without NAF1 or GAR1, can bind an H/ACA RNA (42, 45). *In vivo* this assembly depends on NAF1 and additional H/ACA RNP biogenesis factors including the polymerase II (Pol II)-associated protein NUFIP and RNA/RNP remodeling enzymes such as the helicase-domain proteins RUVBL1/PONTIN and RUVBL2/REPTIN (24). Extensive chaperoning of the H/ACA RNP assembly process may account for the technical barrier to eukaryotic core heterotrimer reconstitution as intact RNP. No high-resolution structural studies have been successful for the complete eukaryotic core heterotrimer; only structures of protein complexes lacking NHP2 have been very recently described (28, 29).

Archaeal pseudouridylation guide RNAs bind dyskerin, NOP10, and an NHP2-related protein, L7Ae, but unlike the eukaryotic RNAs, they can autonomously assemble a single-hairpin

Received 1 March 2012 **Returned for modification** 9 April 2012
Accepted 12 April 2012
Published ahead of print 23 April 2012
Address correspondence to Kathleen Collins, kcollins@berkeley.edu.

doi:10.1128/MCB.00286-12

RNP (9). High-resolution structures of reconstituted single-stem archaeal RNP assemblies reveal that the archaeal ortholog of dyskerin contacts a large RNA surface spanning the ACA, lower hairpin stem, and 3′ side of the pocket (12, 27, 30). RNA structural requirements to maintain this contact surface rationalize the conserved 14- to 16-nt spacing of an H box or ACA from the apex of the preceding hairpin pocket. In contrast to dyskerin, which has an evolutionarily conserved RNA binding specificity, the RNA binding specificity of archaeal L7Ae is different from that of eukaryotic NHP2: L7Ae recognizes a defined kink-turn motif, while NHP2 shows weaker general RNA binding activity (21, 25, 35). Accordingly, L7Ae binds RNA dependent only on RNA sequence while the RNA binding specificity of NHP2 derives from its assembly with other eukaryotic H/ACA proteins.

All known vertebrate pseudouridylation guide RNAs are 5′ and 3′processed from introns of host mRNAs (24). In contrast, vertebrate telomerase RNAs are unspliced transcripts of Pol II that must be only 3′ processed to the hTR H/ACA domain boundary (17, 32–33, 41). The template-containing hTR 5′ extension is not removed and instead gains a trimethylguanosine cap added by the nuclear (short) form of the methyltransferase TGS1 (15, 19, 32). RNP biogenesis steps required for hTR maturation but not for maturation of intron-encoded human H/ACA RNAs could explain why hTR accumulation is uniquely affected by H/ACA protein gene mutations that underlie diseases such as the bone marrow failure syndrome dyskeratosis congenita (DC). X-linked DC patient cells that express a variant dyskerin have reduced levels of hTR and prematurely short telomeres, but they show little, if any, general change in H/ACA snoRNAs and scaRNAs (2, 34, 46). Here, we describe the mechanism by which hTR sequence features distinguish H/ACA RNP assembly on hTR from assembly of the same RNP on other human H/ACA RNAs. Instead of a difference in the pathway of RNP assembly, we find that hTR-specific *in vivo* requirements for RNP assembly act to stimulate a common, direct step of RNA-protein interaction. Our findings have implications for the specialized assembly requirements of hTR versus other H/ACA RNAs and for the mechanism of eukaryotic H/ACA RNP assembly in general.

MATERIALS AND METHODS

Cell culture and expression constructs. Human 293T and HeLa cells were cultured in Dulbecco's modified Eagle's medium (DMEM) with 10% fetal bovine serum and transiently transfected using the calcium phosphate method and lipofection with Lipofectamine (Invitrogen), respectively. The pBS-U3-hTR-500 and pBS-U3-hTR H/ACA-500 expression constructs for mature hTR and the hTR H/ACA domain, the snoRNA expression vectors pBS-U3-U64-500 and pBS-U3-ACA28-500, and the *Tetrahymena* TER transfection control (TC) expression construct have been previously described (13, 17). Hammerhead and hepatitis delta virus self-cleavage motifs were used as previously published (3, 10). Tagged proteins were expressed as N-terminal fusions in a pcDNA-ZZ-TEV (where ZZ represents two IgG binding domains from protein A and TEV is tobacco etch virus protease cleavage site) or pcDNA-ZZ-TEV-calmodulin binding peptide (pcDNA-TAP) plasmid backbone. *In vitro* transcription templates were constructed by cloning DNA sequences encoding a full-length RNA or 3′ hairpin into the PvuII site of pBluescript with retention of the PvuII site at the 3′ end. The *Pseudomonas* phage 7 (PP7)-tagged RNAs harbor PP7 hairpin sequence (6) and a linker (AGUC) followed by the hTR 3′ hairpin sequence. All constructs were verified by sequencing.

Blot detection of RNA and protein. RNA was purified using TRIzol according to the manufacturer's protocol (Invitrogen). For analysis of total RNA, 10 to 20 μg was loaded on a 5% or 6% acrylamide–7 M urea–0.6× TBE (Tris-borate-EDTA) gel. Northern blotting was performed as previously described, using end-labeled complementary oligonucleotides as probes (13, 17). The hTR H/ACA domain was detected using an end-labeled DNA probe complementary to nt 371 to 398; the ACA28 probe was complementary to nt 79 to 107, and the U64 probe was complementary to nt 54 to 72. Northern blots were imaged using a Typhoon Trio phosphorimaging system (GE Healthcare). Quantification of hybridization signal intensity was adjusted for background and then normalized relative to the relevant control signal in the same lane. Immunoblots to verify tagged protein expression (data not shown) used rabbit IgG primary antibody (Sigma) and were imaged using a Li-Cor Odyssey system.

RNA synthesis and purification. RNAs were generated using T7 RNA polymerase and PvuII-digested plasmid templates. Radiolabeling was performed by incorporation of [^{32}P]UTP (NEN/Perkin Elmer). RNAs were resolved by electrophoresis on a 6% acrylamide–7 M urea–0.6× TBE gel, excised from the gel, and eluted in 0.3 M sodium acetate overnight at 37°C, followed by ethanol precipitation. The concentrations of purified RNAs were determined by absorbance, and their quality was verified by electrophoresis and SYBR gold staining or autoradiography.

RNP assembly in extract. RNP assembly was performed in 10-μl reaction mixtures containing ~20 μg of HeLa whole-cell extract total protein obtained from freeze-thaw lysis in a final buffer of 20 mM HEPES at pH 8.0, 2 mM $MgCl_2$, 0.2 mM EGTA, 10% glycerol, 0.1% Igepal, 0.1 mM phenylmethylsulfonyl fluoride (PMSF), 100 mM NaCl, 5 mM dithiothreitol (DTT), 0.25 μl of RNasin (Promega), 500 ng of yeast tRNA (Sigma), and loading dyes. Approximately 50 pg of radiolabeled RNA probe was added, and reaction mixtures were incubated at 30°C for 1 h, followed by a 10-min chase with 1.5 μg of heparin. Cold competitor RNAs were preincubated at 30°C for 30 min in the presence of all components except radiolabeled RNA. RNP complexes were resolved by electrophoresis on a 5% acrylamide–0.5× TBE gel at 4°C. Gels were dried and imaged using the Typhoon Trio.

RNP assembly and detection of radiolabeled RNA. For affinity purification of RNPs using a tagged protein, cell extracts from freeze-thaw lysis were diluted to ~2.5 mg/ml in binding buffer (20 mM HEPES at pH 8.0, 100 mM NaCl, 2 mM $MgCl_2$, 0.2 mM EGTA, 10% glycerol, 0.1% Igepal, 1 mM DTT, 0.1 mM PMSF). A 100- to 150-μl volume of diluted extract was clarified by centrifugation and adjusted to a final concentration of 5 mM DTT and supplemented with 0.5 μl of RNasin. The extract was incubated at 30°C for 20 to 30 min with ~5 ng of radiolabeled RNA. Then 2.5 μl of packed IgG agarose (Sigma) prewashed in 1 ml of binding buffer was added, and samples were rotated end over end for 1 to 2 h at 4°C. Alternatively, the IgG agarose purification and RNA incubation steps were reversed, with a single wash at room temperature in 1 ml of binding buffer for 5 min and resuspension of the resin in 50 μl of binding buffer plus 100 ng/μl bovine serum albumin in between. Bound RNPs were washed three times at room temperature in 1 ml of wash buffer [binding buffer with 0.1% Triton X-100 and 0.1% CHAPS {3-[(3-cholamidopropyl)-dimethylammonio]-1-propanesulfonate)} for 5 min each wash. Buffer was removed, and the resin was resuspended in formamide with EDTA and loading dye and then boiled for 5 min. The supernatant was loaded on a 6% acrylamide–7 M urea–0.6× TBE gel. Gels were dried and imaged using the Typhoon Trio.

Cellular RNP affinity purification. For affinity purification of ZZ-tagged NHP2 RNPs assembled *in vivo*, cell extracts from freeze-thaw lysis were diluted to ~0.75 mg/ml in binding buffer as above with 150 mM NaCl. A 900-μl volume of diluted extract was clarified by centrifugation immediately prior to purification using 2.5 μl of prewashed IgG-agarose. Samples were rotated end over end for 2 h at 4°C and then washed three times at room temperature in 1 ml of wash buffer for 5 min each wash. To elute bound RNPs, ~30 ng/μl of the S219V variant of tobacco etch virus protease was added in a volume of 50 μl of elution buffer (wash buffer with 100 ng/μl bovine serum albumin and 100 ng/μl tRNA), and samples were rotated end over end for 30 min at room temperature.

RESULTS

The hTR BIO box functions in collaboration with consensus elements of the H/ACA motif. The biological accumulation of hTR but not any other studied human H/ACA RNA depends on a sequence motif in the loop of the 3′ hairpin (Fig. 1A). The 3′ half of this hTR loop contains the biogenesis-promoting box (the BIO box) important for mature RNA accumulation, while the 5′ half of the loop contains a CAB (Cajal body) box dispensable for RNA accumulation but required for mature RNP concentration in Cajal bodies (17, 23, 41). Function of both the BIO box and the CAB box depends on the integrity of the adjacent stem, and disruption of this stem imposes autosomal dominant DC (44). Previously assayed BIO box sequence substitutions that eliminated mature hTR accumulation either replaced the entire loop or severely disrupted loop structure by introducing additional base pairing (17, 41). In search of a minimal change that selectively disrupts BIO box function without altering the length of the 3′ hairpin stem, we assayed additional sequence variants for their impact on mature hTR accumulation.

We expressed hTR precursor using the Pol II expression construct U3-hTR-500, which contains the U3 C/D box snoRNA promoter, mature hTR sequence, and 500 bp of downstream sequence from the endogenous locus. This construct efficiently produces 3′ processed hTR that is incorporated into the biologically active telomerase holoenzyme (17, 46). Total RNA was harvested from transfected human 293T cells, resolved by denaturing polyacrylamide gel electrophoresis (PAGE), and probed by Northern blotting to detect the accumulation of hTR and an internal loading control (LC). As demonstrated previously, the disruption of CAB box function with the substitution G414C did not inhibit mature hTR accumulation, while deletion of the 3′ hairpin upper stem-loop or loop replacement with a structured tetraloop reduced hTR accumulation to a level undetectable over the background of endogenous hTR in cells transfected with empty vector (Fig. 1B, lanes 1 to 3 and 8 to 9; note that mature hTR often migrates as a doublet due to partial folding). To reduce loop interaction with CAB box binding proteins for purposes of the RNP assembly assays described below, we subsequently included the G414C CAB box substitution in "wild-type" hTR unless indicated otherwise.

Vertebrate telomerase RNAs share absolute conservation of the final loop residue that is hTR U418 (Fig. 1A) and >85% conservation of the preceding guanosine that is hTR G417 (37). The nuclear magnetic resonance (NMR) structure of a model hTR 3′ hairpin stem-loop suggests that G417 pairs with U411 (41). Although the G417C substitution strongly reduced hTR RNP accumulation monitored by RNase protection (41), replacement of G417 with adenosine had little impact (Fig. 1B, lane 4), perhaps because A-U base pairing would still be possible. In contrast, replacement of the absolutely conserved U418 with cytidine strongly reduced mature hTR accumulation (Fig. 1B, lane 5). The combination of these two substitutions was no more deleterious than the U418C substitution alone (Fig. 1B, lane 6). Replacing the entire 3′ hairpin loop with the U17 snoRNA 3′ hairpin loop CUGUC, which contains the BIO box sequence with an extra 3′ cytidine, did not provide full BIO box function (Fig. 1B, lane 7). Because the U418C substitution substantially reduced mature hTR accumulation *in vivo* without changing 3′ hairpin stem or

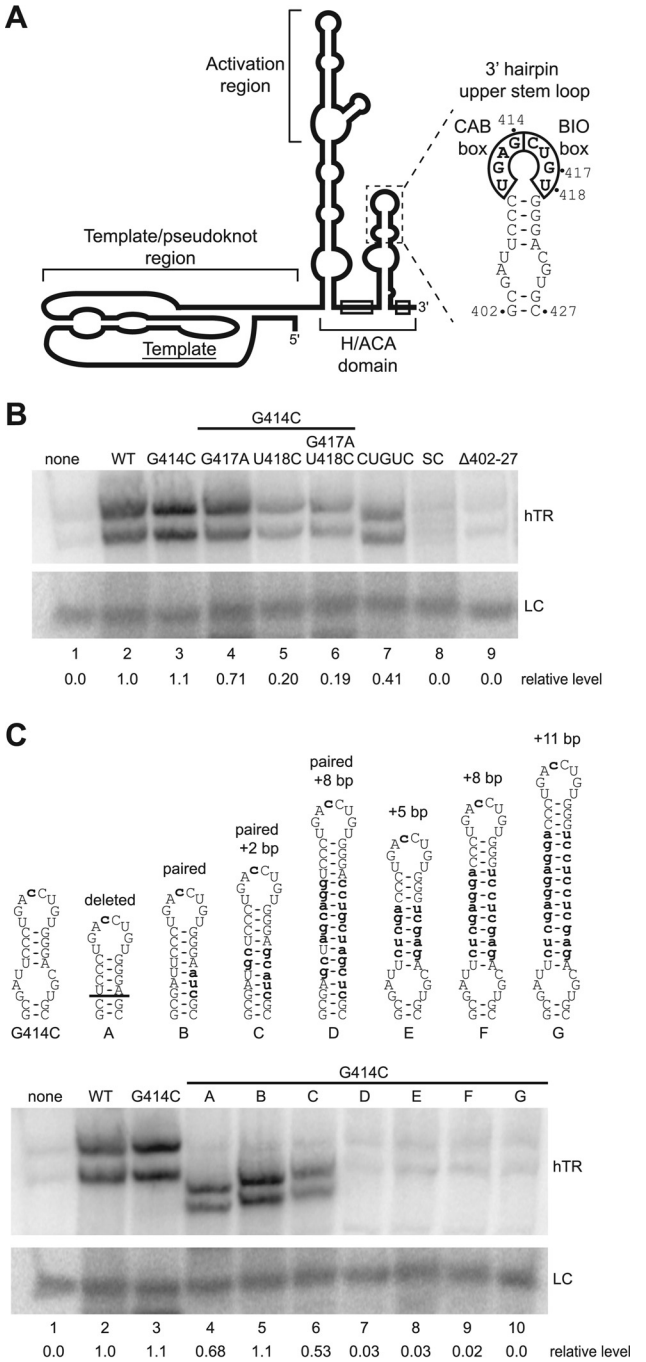

FIG 1 The BIO box has sequence and positioning requirements for function. (A) Secondary structure of full-length hTR and primary sequence of the 3′ hairpin upper stem-loop. Open boxes within the H/ACA domain indicate the location of the H box and ACA (left and right boxes, respectively). (B and C) BIO box sequence and positioning requirements. Total RNA from transfected cells was examined by Northern blot hybridization for recombinant wild-type (WT) hTR or the hTR variants indicated, as well as for an endogenous cross-hybridizing RNA (LC) detected in parallel on the same blot. Cells transfected with an empty expression vector provided an endogenous hTR background control (lanes labeled none). The CUGUC mutation replaces the entire loop sequence with that of the 3′ hairpin loop of the human U17 snoRNA. The stem cap (SC) mutation replaces the entire loop with a GAAA tetraloop. In panel C, base pairing and length of the 3′ hairpin upper stem were altered as indicated by bold font and lowercase lettering in the illustrations for variant stems A to G, with a line indicating the internal loop deletion in variant A. Values below the lane numbers are loading-normalized accumulation levels relative to wild type.

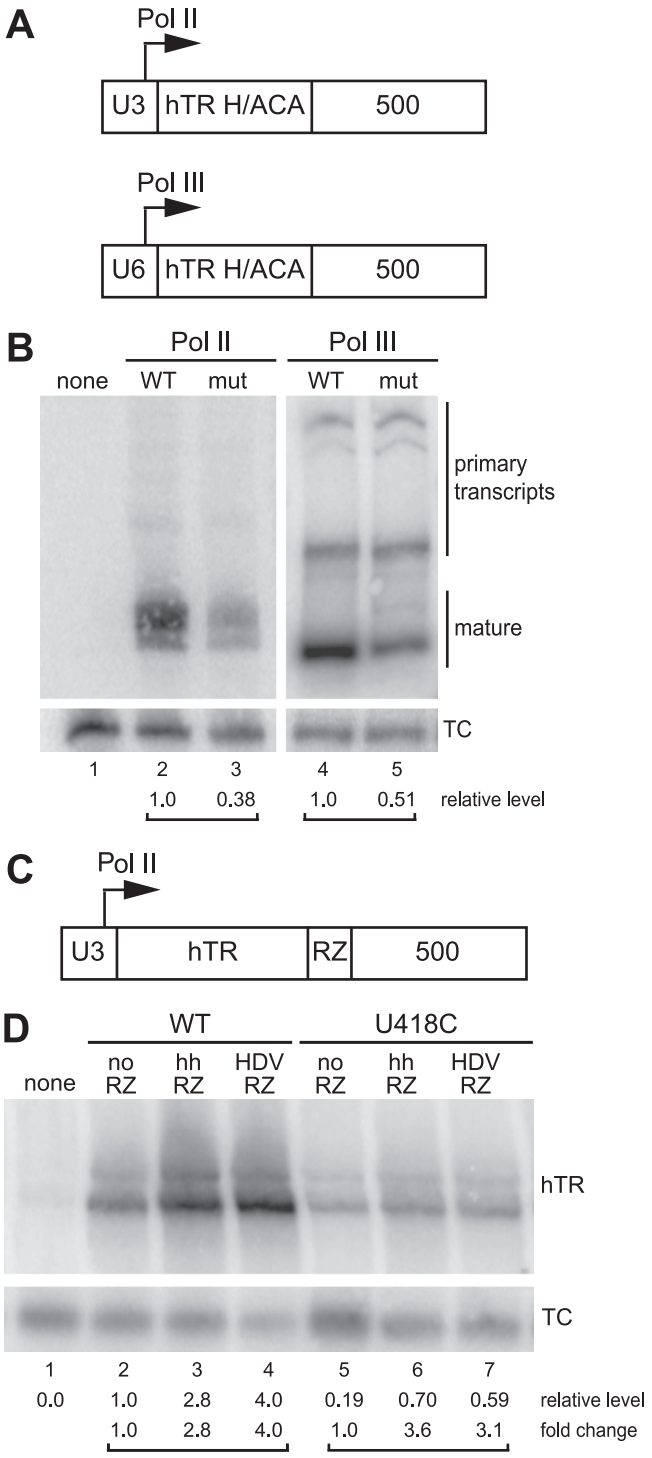

FIG 2 The BIO box enhances RNP accumulation in different transcription contexts. (A and B) Construct schematics and results for BIO box function in Pol II and Pol III expression contexts. The hTR H/ACA domain (nt 203 to 451) with a wild-type (WT) 3′ hairpin loop or the CAB box/BIO box G414C/U418C double mutation (mut) was expressed using the promoter of human U3 or U6. Relative accumulation values were quantified using the signal intensities of the fastest-migrating, 3′-processed RNAs (with potential additional 5′ processing of a few nucleotides for transcripts of Pol III), first normalized to the transfection control (TC) and expressed relative to the corresponding wild-type RNA. (C and D) Schematic of hTR RZ expression constructs and RZ impact on hTR accumulation. WT or U418C hTR backbone was assayed in parallel without the RZ (lanes 2 and 5) or with the minimal hammerhead (hh) or hepatitis delta virus (HDV) RZ inserted 10 nt after the mature hTR 3′ end. Accumulation values were normalized to the transfection control (TC) and are expressed relative to the U3-hTR-500 construct (numbers given directly below lane numbers). Fold stimulation by ribozyme insertion was also calculated (numbers in bottom rows).

loop length, we used this substitution for BIO box disruption in subsequent studies.

Surprisingly, it has not been addressed whether the BIO box functions autonomously or in coordination with the H/ACA motif. To investigate potential positioning-dependent coordination between the BIO box and the H/ACA motif, we altered or extended 3′ hairpin base pairing in the upper stem (Fig. 1C). We found that deleting or pairing a predicted internal loop in the upper stem did not severely inhibit mature hTR accumulation (Fig. 1C, lanes 3 to 5). In contrast, insertion of additional base pairs in the upper stem reduced mature hTR accumulation in proportion to the increase in stem length: insertion of two base pairs only partially inhibited hTR accumulation, while the insertion of eight base pairs reduced hTR accumulation to a level undetectable above background (Fig. 1C, lanes 6 to 7). Similar inhibition of mature hTR accumulation was observed when five or eight base pairs were added to a 3′ hairpin upper stem that retained the wild-type internal loop (Fig. 1C, lanes 8 and 9). Accumulation was not restored by insertion of 11 base pairs, which would present the BIO box on the same helical face as in wild-type hTR (Fig. 1C, lane 10). We also attempted to functionally transplant an ectopic BIO box to other positions of mature or precursor hTR without achieving a rescue of the accumulation defect imposed by U418C substitution of the native BIO box (data not shown). Together, these results suggest that the physical spacing between the BIO box and the 3′ hairpin pocket is critical for BIO box function.

BIO box function does not require Pol II-coupled precursor expression or 3′ end formation. The BIO box remains critical for RNA accumulation even if the noncanonical hTR H/ACA motif is swapped for a canonical H/ACA snoRNA (17). However, BIO box function is not required if the hTR H/ACA domain accumulates by processing from a spliced intron rather than an unspliced autonomous transcript (41). Together, these findings suggested that BIO box function is coupled to transcription context. This hypothesis has support from precedent because transcription-coupled association of processing factors with nascent yeast H/ACA snoRNA transcripts determines their specificity of 3′ end formation and processing as snoRNAs (40).

To investigate whether BIO box function is dependent on hTR H/ACA domain expression as an autonomous transcript of Pol II, we compared the BIO box dependence of hTR H/ACA domain accumulation in a Pol II versus Pol III expression context (Fig. 2A). Pol III does not support the synthesis of full-length hTR due to the presence of internal polyuridine tracts (32). Therefore, the U3-hTR H/ACA-500 expression vector, which includes only the hTR H/ACA domain (nt 203 to 451), was minimally altered to create U6-hTR H/ACA-500, which replaces the human U3 C/D-box snoRNA Pol II promoter with the human U6 small nuclear RNA Pol III promoter. The hTR H/ACA domain has been shown to be 5′ and 3′processed from a full-length hTR transcript *in vivo* (33). As expected from previous work, BIO box mutation reduced hTR H/ACA domain accumulation from the Pol II-transcribed

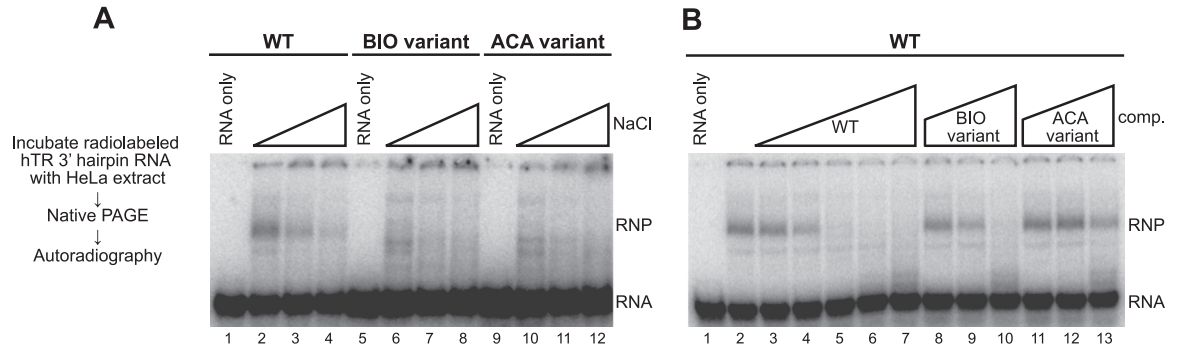

FIG 3 The BIO box stimulates RNP assembly on the hTR 3′ hairpin. Radiolabeled hTR 3′ hairpin probes were added to HeLa whole-cell extract with RNP assembly monitored by EMSA. In panel A, wild-type (WT) RNA corresponds to nt 381 to 451 of hTR variant B shown in Fig. 1C, in which the upper stem internal loop is paired and the CAB box is disrupted by the G414C substitution. BIO variant RNA harbors an additional U418C substitution, while ACA variant RNA has the substitution ACA446-UGU448. The concentration of NaCl was 100, 200, or 300 mM. In panel B, RNP assembly on WT RNA was challenged by preaddition of unlabeled WT competitor RNA (comp) at a final concentration of 0.01 ng/μl to 100 ng/μl or unlabeled BIO or ACA variant RNA at a final concentration of 1 ng/μl to 100 ng/μl in 10-fold steps.

precursor (Fig. 2B, lanes 1 to 3). Unexpectedly, BIO box mutation also reduced the accumulation of a Pol III-transcribed RNA that migrates with the mobility expected for a properly 5′- and 3′-processed hTR H/ACA domain (Fig. 2B, lanes 4 and 5). Based on blot hybridization results (data not shown), longer RNAs produced by Pol III are likely to be polyuridine-terminated primary transcripts protected from 3′-end trimming by La protein. We conclude that although the efficiency of processing is affected by transcription context, the BIO box can promote hTR H/ACA RNP accumulation independent of the transcribing polymerase and its associated factors.

Even if forced to be uncoupled from primary transcript synthesis, the BIO box could still function to recruit productive 3′-end processing machinery. For example, the BIO box could promote endonucleolytic cleavage of the primary transcript to override polyadenylation-induced nuclear export or degradation. This model has the appeal of accounting for a complete lack of a recognizable or required 3′ end formation signal downstream of mature hTR at its genomic locus (15, 17, 32). We tested this model by inserting a self-cleaving ribozyme (RZ) after the 3′ end of mature hTR in an attempt to rescue the accumulation defect imposed by BIO box mutation (Fig. 2C). We inserted either a minimal hammerhead RZ or a hepatitis delta virus RZ, the latter of which is reported to undergo particularly rapid cotranscriptional cleavage (16). Surprisingly, although either RZ improved the accumulation of wild-type or BIO box mutant hTR, neither rescued the relative accumulation deficit imposed by BIO box disruption (Fig. 2D, compare lane 2 to lanes 3 and 4 and lane 5 to lanes 6 and 7 as well as lanes 2 to 4 to lanes 5 to 7). These findings suggest that the formation or persistence of a precursor 3′ end can be rate limiting for hTR accumulation, such that RZ self-cleavage and/or formation of a nuclease-resistant 2′3′-cyclic phosphate promotes mature hTR production. In addition, toward understanding the role of the BIO box, the findings above indicate that the hTR functional requirement for a BIO box is independent of the precursor 3′ end formation mechanism.

The BIO box promotes hTR 3′ hairpin RNP assembly. Instead of acting at an hTR-specific step of RNA processing, the BIO box could act at an early RNP assembly step by directly binding to a recruiting factor for H/ACA proteins. In this scenario, the hTR-specific requirement for the BIO box would derive from the need for hTR RNP assembly to compete with the more rapid degradation of its precursor relative to intron-encoded H/ACA RNA precursors, which would be protected from exonucleolytic degradation within a host mRNA transcript. Consistent with the hypothesis above, RNP assembly monitored by electrophoretic mobility shift assay (EMSA) indicated that HeLa cell extract assembled a distinct complex on the hTR H/ACA domain in addition to the complexes formed by both hTR and H/ACA snoRNAs (11). The hTR 3′ hairpin with a wild-type CAB box and BIO box (both uncharacterized at the time) could compete for RNP assembly on the entire hTR H/ACA domain (11). We therefore used HeLa whole-cell extract to determine whether the BIO box has a stimulatory role in RNP assembly on a pretranscribed RNA. We used radiolabeled hTR 3′ hairpin with the internal loop of the upper stem paired to promote stable folding (variant B in Fig. 1C) and with the CAB box disruption G414C to inhibit loop binding by the proteins that mediate Cajal body localization. RNA containing only these substitutions was the wild-type backbone for BIO box disruption by U418C substitution or ACA disruption by trinucleotide replacement with UGU (BIO and ACA variants, respectively).

When incubated with HeLa whole-cell extract, the reference wild-type hTR 3′ hairpin assembled an RNP with a discrete shift in electrophoretic mobility (Fig. 3A, lanes 1 to 2). This RNP assembly was sensitive to increasing salt concentration but was still detectable in the presence of 300 mM NaCl (Fig. 3A, lanes 2 to 4). RNPs assembled by the BIO and ACA variant RNAs migrated faster than RNPs assembled on the wild-type RNA and were nearly eliminated by only 200 mM NaCl (Fig. 3A, lanes 6 to 8 and 10 to 12). Disruption of the salt-stable RNA mobility shift by BIO box or ACA mutation suggested that the BIO box could have a role in promoting RNP assembly.

To better compare the relative RNP assembly efficiencies of the wild-type versus BIO and ACA variant RNAs, we measured the ability of unlabeled competitor RNAs to inhibit RNP assembly on the radiolabeled wild-type RNA (Fig. 3B). Various concentrations of unlabeled competitor RNA were preincubated with whole-cell extract and other buffer components before radiolabeled wild-type 3′ hairpin RNA was added. Unlabeled wild-type RNA inhibited RNP assembly to half-maximum at a concentration of 0.1 ng/μl, an approximately 20-fold excess over the limiting radiola-

beled RNA (Fig. 3B, lane 4). In contrast, BIO box mutant RNA at over 2,000-fold excess or ACA mutant RNA at over 20,000-fold excess was required to achieve half-maximal inhibition (Fig. 3B, lane 9 or 13). We conclude that the U418C BIO box mutation reduced hTR 3′ hairpin RNP assembly efficiency significantly but to a lesser extent than mutation of the ACA motif. This parallels the impact of BIO box or ACA mutation on hTR accumulation *in vivo*.

The BIO box promotes direct H/ACA protein-RNA interaction. The BIO box and ACA dependence of RNP assembly on a pretranscribed RNA suggested that whole-cell extract reconstituted a physiological H/ACA RNP complex, but this was not conclusively established by EMSA alone. To further investigate the nature of the RNP assembled in whole-cell extract, we used extracts from HeLa cells overexpressing a protein of interest N-terminally tagged by fusion to tandem IgG binding domains (the ZZ tag). All tagged proteins used here were robustly and comparably overexpressed in transfected cells, as quantified by immunoblotting of whole-cell extract (data not shown). After radiolabeled RNA incubation in cell extract, RNPs containing the tagged protein were recovered on IgG resin, washed, and quantified using denaturing PAGE. In this assay, the amount of recovered radiolabeled RNA indicates the success of its assembly into RNP complexes containing the protein of interest.

We first applied this approach to the H/ACA RNP proteins dyskerin, NHP2, and GAR1 (NOP10 is refractory to tagging, but since it is the bridge between dyskerin and NHP2, its presence can be inferred). To reduce extract-mediated degradation of the radiolabeled RNA during affinity purification, we tagged the hTR 3′ hairpin at its 5′ end with the *Pseudomonas* phage 7 (PP7) stem-loop binding site for coat protein (22), which we found to stabilize the recombinant RNA in extract even without added PP7 coat protein. Dyskerin, NHP2, and GAR1 all assembled on the hTR 3′ hairpin, with an efficiency reduced by BIO box mutation and abrogated entirely by ACA mutation (Fig. 4A). Cell extract containing no tagged protein was used as a specificity control (Fig. 4, lanes 13 to 15). Similar results were obtained using untagged hTR 3′ hairpin RNAs (data not shown). We also verified that this specificity was not due to enhanced degradation of the BIO and ACA variant RNAs in extract, as judged by equal recovery of radiolabeled RNAs from the unbound extract fraction following RNP affinity purification (data not shown). We conclude that the BIO box strongly stimulates H/ACA RNP assembly on the hTR 3′ hairpin in whole-cell extract.

We then modified the reconstitution assay, reversing the immunopurification and RNA incubation steps. The tagged protein alone and any complexes containing the tagged protein were isolated by binding to IgG resin, washed resin was incubated with radiolabeled RNA, and, after removal of free RNA with additional washes, any RNP-assembled RNA was recovered and resolved by denaturing PAGE. In this assay, complexes containing tagged dyskerin or NHP2 but not GAR1 could assemble on the hTR 3′ hairpin, and this assembly was reduced by BIO box mutation and eliminated by ACA mutation (Fig. 4B). Because GAR1 joins an H/ACA RNP late in its maturation, our RNP assembly assay with prepurified complexes recapitulates the physiological specificity of H/ACA RNP assembly: GAR1 should not purify an RNA-free protein complex that can load recombinant RNA, but if RNA is assembled into RNP in extract, additional maturation steps including the recruitment of GAR1 can occur.

We next examined the specificity of NAF1 interaction. Tagged NAF1 copurified the hTR 3′ hairpin RNA following RNP assembly in extract (Fig. 4C, lanes 7 to 9), and prepurified protein complexes with tagged NAF1 bound RNA directly (Fig. 4D, lanes 7 to 9). In either case, RNP formation was strongly reduced by BIO box mutation and eliminated by ACA mutation. Overall, the findings above indicate that NAF1, dyskerin, NHP2, and, by extension, NOP10 form a preassembled protein complex that is capable of binding the hTR 3′ hairpin. Also, at least under our extract RNP assembly conditions, the exchange of NAF1 for GAR1 remains incomplete. More surprisingly, BIO box-dependent hTR RNP reconstitution with purified, NAF1-bound core proteins suggests that the BIO box binding partner is part of this preassembled protein scaffold.

The preassembled core protein scaffold lacks other known chaperones. Cellular biogenesis of H/ACA RNPs requires numerous factors, in addition to NAF1, that interact with dyskerin, NOP10, and/or NHP2 and assist in the RNA processing and RNP assembly steps preceding formation of a mature RNP. To evaluate whether these factors associate with RNP assembled in extract or, of special interest, form part of the preassembled NAF1/dyskerin/NOP10/NHP2 scaffold competent for direct RNA binding, we expressed tagged versions of known H/ACA RNP biogenesis factors and assayed their hTR interaction using both reconstitution protocols. Assembly of radiolabeled hTR 3′ hairpin in extract followed by RNP purification detected BIO box and ACA-dependent interaction of two more RNP assembly chaperones: NUFIP and RUVBL2 (Fig. 4C, lanes 4 to 6 and 10 to 12). Similar assays of additional factors required for hTR biogenesis *in vivo*, including the nuclear cap methyltransferase sTGS1 (Fig. 4C, lanes 13 to 15), failed to detect associations with the extract-assembled hTR 3′ hairpin RNP.

Notably, neither NUFIP nor RUVBL2 was part of the preformed protein scaffold competent for direct RNA binding (Fig. 4D, lanes 4 to 6 and 10 to 12). Assays of additional factors required for hTR biogenesis *in vivo*, including sTGS1 (Fig. 4D, lanes 13 to 15), also did not copurify the assembly-competent protein scaffold. Despite many years of investigation, it remains possible that some H/ACA RNP assembly factors remain to be discovered, but the most likely explanation to account for the results above is that a scaffold containing only NAF1, dyskerin, NOP10, and NHP2 is the platform for direct binding to an H/ACA RNA precursor. Other biogenesis factors that associate with an H/ACA RNP reconstituted in cell extract are not part of this assembly-competent scaffold prior to RNA loading. Furthermore, because hTR association with the preassembled protein scaffold remains dependent on the BIO box even when the scaffold is purified from extract prior to RNP assembly, the scaffold itself provides the BIO box-dependent RNP assembly stimulation.

No high-resolution structure of a eukaryotic core heterotrimer is available, with or without bound RNA. Of the core heterotrimer proteins, only NHP2 would be positioned suitably for direct contact with the BIO box (20, 24). Consistent with results from a previous study of yeast Nhp2p (21), we find that recombinant human NHP2 alone binds the hTR 3′ hairpin without specificity for the BIO box (data not shown). A measurable sequence preference of NHP2 binding is likely to require its structural constraint by protein-protein interaction(s). We suggest that protein preassembly to form the NAF1/dyskerin/NOP10/NHP2 scaffold biases the conformational heterogeneity observed in recent solution

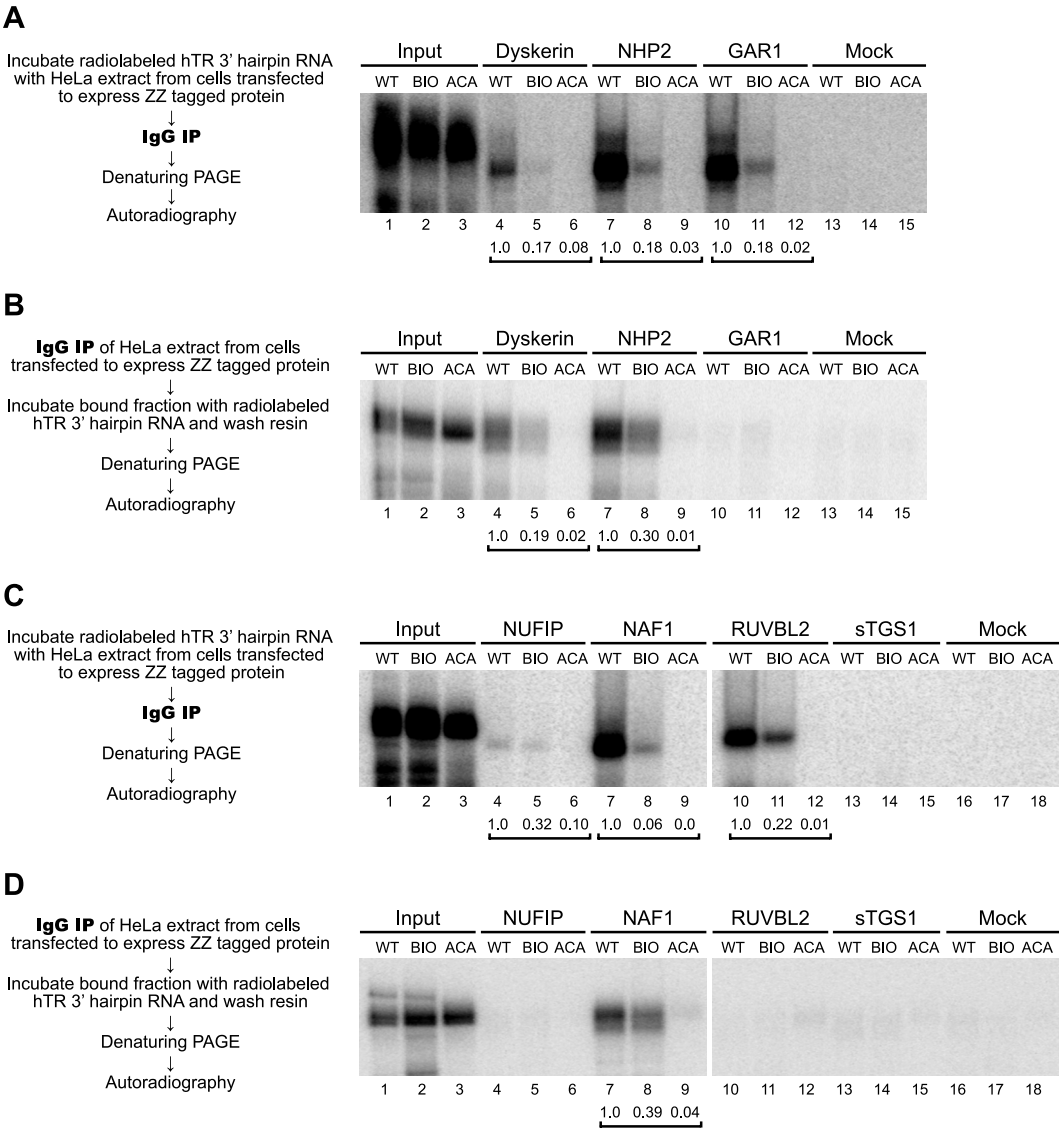

FIG 4 RNP assembly specificity is recapitulated with a purified protein scaffold. (A and C) HeLa whole-cell extracts from cells transfected to express the indicated ZZ-tagged protein or untransfected cells (Mock) were incubated with radiolabeled PP7-tagged hTR 3′ hairpin probe (WT or the BIO or ACA variant). Following RNP immunopurification on IgG resin and washing to remove unbound RNA, bound RNA (100%) was detected relative to input RNA (2%). (B and D) Complexes containing the indicated ZZ-tagged protein were immunopurified from whole-cell extract of transfected HeLa cells prior to incubation with a radiolabeled PP7-tagged hTR 3′ hairpin RNA. Following washing to remove unbound RNA, bound RNA (100%) was detected relative to input RNA (2%). Values below lane numbers are the input-normalized quantification of bound BIO or ACA RNA relative to WT RNA within each bracketed set. IP, immunoprecipitation.

structures of isolated yeast Nhp2p (26) to favor the NHP2 conformation with a binding preference for the loop uridine presented by the hTR BIO box.

The preassembled core protein scaffold supports concerted two-hairpin RNP assembly. Results above demonstrate that hTR H/ACA RNP assembly is dependent on the hTR BIO box *in vitro* as well as *in vivo*, but other human H/ACA RNAs lack this motif. To investigate the *in vitro* RNP assembly properties of other human H/ACAs in comparison to hTR, we created a panel of one- or two-hairpin RNAs based on the validated secondary structures of the human U17, U64, and ACA28 snoRNAs (5, 18, 47). U17 is the only human H/ACA RNA known to function in rRNA precursor cleavage rather than pseudouridylation, and it is the only known individually essential H/ACA RNA in yeast (24). Like hTR, U17 has a noncanonical 5′ hairpin structure and a 3′ hairpin that can compete for full-length U17 RNP assembly in HeLa nuclear extract (11).

We first assayed RNP assembly in extract for the radiolabeled two-hairpin U17, U64, and ACA28 snoRNAs and a comparably snoRNA-sized version of hTR (Fig. 5A), which lacks the 5′ hairpin extension for telomerase catalytic activation (Fig. 1A). We also assayed RNP assembly on the single 3′ hairpin of each snoRNA. The two-hairpin and 3′ hairpin hTR and U17 RNAs each assembled an H/ACA RNP in extract, as monitored by postassembly purification of tagged NHP2 (Fig. 5A, lanes 8, 9, 11, 13, and 14). In contrast, although the two-hairpin versions of U64 and ACA28

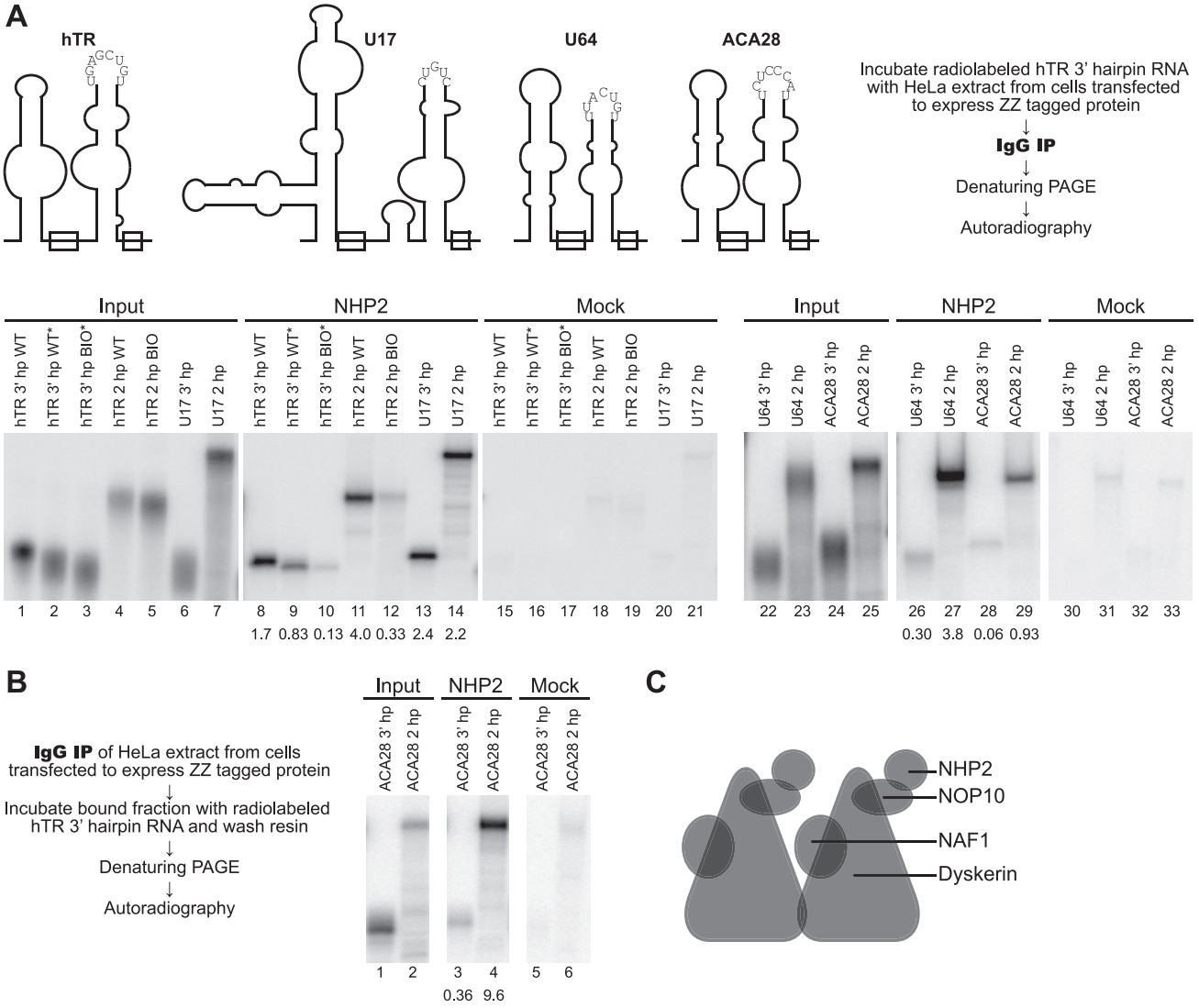

FIG 5 Pseudouridylation guide RNAs show concerted two-hairpin RNP assembly. (A) HeLa whole-cell extracts from cells transfected to express ZZ-tagged NHP2 were incubated with radiolabeled 3′ hairpin (hp) or two-hairpin hTR (WT or BIO variant), U17, U64, or ACA28. The snoRNA-sized version of hTR used as the two-hairpin RNA is depicted. An asterisk indicates RNAs in which the internal loop of the hTR 3′ hairpin was paired. Following RNP immunopurification and washing to remove unbound RNA, bound RNA (100%) was detected relative to input RNA (2%). Values below lane numbers are percentages of input RNA bound. (B) Complexes containing ZZ-tagged NHP2 were immunopurified from whole-cell extract prior to incubation with radiolabeled 3′ hairpin or two-hairpin ACA28 RNA. Following washing to remove unbound RNA, bound RNA (100%) was detected relative to input RNA (2%). Values below lane numbers are percentages of input RNA bound. (C) Model for the subunit composition of a protein scaffold competent for RNA binding. A protein interaction(s) that could putatively dimerize the core proteins is not established; for the sake of illustration, contact between dyskerin subunits is suggested.

assembled an RNP, the 3′ hairpin of either snoRNA alone did not (Fig. 5A, lanes 26 to 29). Notably, the BIO box enhanced RNP assembly even for the snoRNA-like two-hairpin version of hTR (Fig. 5A, compare lanes 9 and 10 and lanes 11 and 12). Parallel controls for background binding used cell extracts with no tagged protein (Fig. 5, mock purification lanes). The isolated 5′ hairpins from hTR, U17, or other snoRNAs failed to assemble an RNP (data not shown). The same results were obtained using tagged dyskerin instead of tagged NHP2 (data not shown).

We next assayed the panel of single-hairpin and two-hairpin RNAs by RNP reconstitution following protein purification. To our surprise, complexes containing tagged NHP2 (Fig. 5B) or tagged dyskerin (data not shown) that were purified prior to RNP assembly supported not only the same specificity of single-hairpin RNP assembly characterized in extract but also robust two-hairpin-dependent RNP assembly (Fig. 5B, lanes 3 and 4). This finding suggests that the purified, resin-immobilized NAF1/dyskerin/NOP10/NHP2 scaffold achieves concerted assembly of core proteins on two H/ACA motif hairpins. Although we cannot exclude some potential for physical association of two separately immobilized NAF1-bound core protein complexes, the results above suggest that the preassembled scaffold for productive RNP assembly could already contain two sets of core proteins (Fig. 5C). This scaffold architecture would account for why eukaryotic H/ACA RNAs all have two hairpins, whereas archaeal RNAs that assemble directly with dyskerin/NOP10 and separately with L7Ae do not.

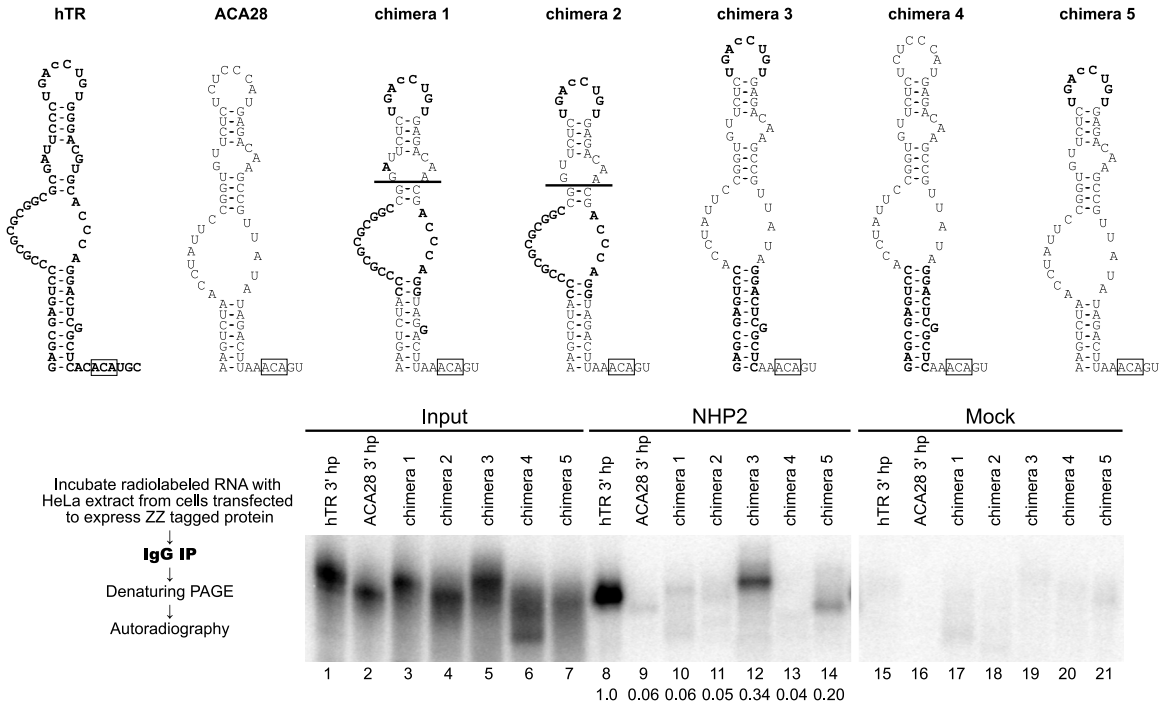

FIG 6 Several hTR 3′ hairpin features contribute to RNP assembly enhancement. HeLa whole-cell extracts from cells transfected to express ZZ-tagged NHP2 were incubated with a radiolabeled hTR 3′ hairpin, ACA28 3′ hairpin, or chimeric hairpin with hTR sequence in bold font. The ACA motif is boxed, and a line indicates a deletion of 2 bp. Following RNP immunopurification and washing to remove unbound RNA, bound RNA (100%) was detected relative to input RNA (2%). Mock purification lanes provide the background binding controls. Values below lane numbers are the input-normalized quantification of bound RNA relative to the hTR 3′ hairpin.

Unfortunately, we found the RNA-binding-competent NAF1/dyskerin/NOP10/NHP2 scaffold to be unstable to stringent washes and/or extended additional purification, hampering direct physical characterization of the functional scaffold architecture.

Distributed features of the hTR 3′ hairpin cooperate to promote RNP assembly. The BIO box alone should contribute only a small fraction of the RNA binding surface for an H/ACA core protein complex, so we considered the possibility that it is necessary but not sufficient for stimulation of hTR 3′ hairpin RNP assembly. We constructed a series of chimeric 3′ hairpin RNAs that contained combinations of elements from hTR and ACA28 (Fig. 6). Chimeras 1 and 2 contained ACA28 sequence with the hTR 3′ loop and also pocket region sequences, including deletion of two base pairs above the pocket and insertion of two base pairs below the pocket to make the stem lengths more similar to those of hTR. In addition, in chimera 1 an adenosine was inserted in the 5′ side of the upper stem and a guanosine was inserted in the 3′ side of the lower stem to make internal loop and bulge sizes identical to hTR. Efficient RNA assembly with H/ACA proteins in extract was not supported by transplant of either the hTR loop or pocket sequences; instead, these chimeric RNAs showed only low, near-background purification similar to the ACA28 3′ hairpin (Fig. 6, lanes 8 to 11). We next transplanted the hTR 3′ hairpin loop and its atypically long lower stem into the ACA28 3′ hairpin backbone to generate chimera 3. The combination of these two hTR elements conferred a robust and reproducible improvement of RNP assembly (Fig. 6, lane 12) that was more than provided by the loop alone (lane 14) or the undetectable RNP assembly with transplant of the lower stem alone (lane 13). Nonetheless, even the combination of loop and lower stem did not fully recapitulate the RNP assembly efficiency of the intact hTR 3′ hairpin (Fig. 6, lane 8). Consistent with the findings above, partially unpairing the 3′ hairpin lower stem to produce a more typical stem length severely reduced mature hTR accumulation *in vivo* (data not shown). An atypically long lower stem could be precluded in modification guide RNAs by competing structural requirements for biological function (see Discussion). These results suggest that multiple features of the hTR 3′ hairpin act in a synergistic manner to increase RNA interaction affinity with the preassembled NAF1-bound core protein scaffold.

Disease-associated H/ACA protein variants affect different steps of RNP assembly. Finally, we investigated a potential connection between hTR sequence-mediated enhancement of H/ACA RNP assembly and the specificity of telomerase deficiency in DC. We overexpressed tagged disease-associated variants of dyskerin and NHP2 in HeLa cells and used the resulting whole-cell extract for reconstitution assays. All of the dyskerin variants supported hTR 3′ hairpin RNP assembly in both reconstitution assays (Fig. 7A and B, lanes 2 to 9). This observation is consistent with the modest, if any, inhibition of RNA binding observed when dyskerin variants were assembled as core heterotrimers in reticulocyte lysate (43, 45). On the other hand, the NHP2 variants imposed severe defects in RNP assembly (Fig. 7A and B, lanes 11 to 13). NHP2 variants expressed by transient transfection of 293T cells showed reduced association with hTR as well as other snoRNAs (Fig. 7C), indicating that their assembly defect is not specific to hTR. These findings also parallel results from studies using reticulocyte lysate for RNP reconstitution (43). Importantly, because

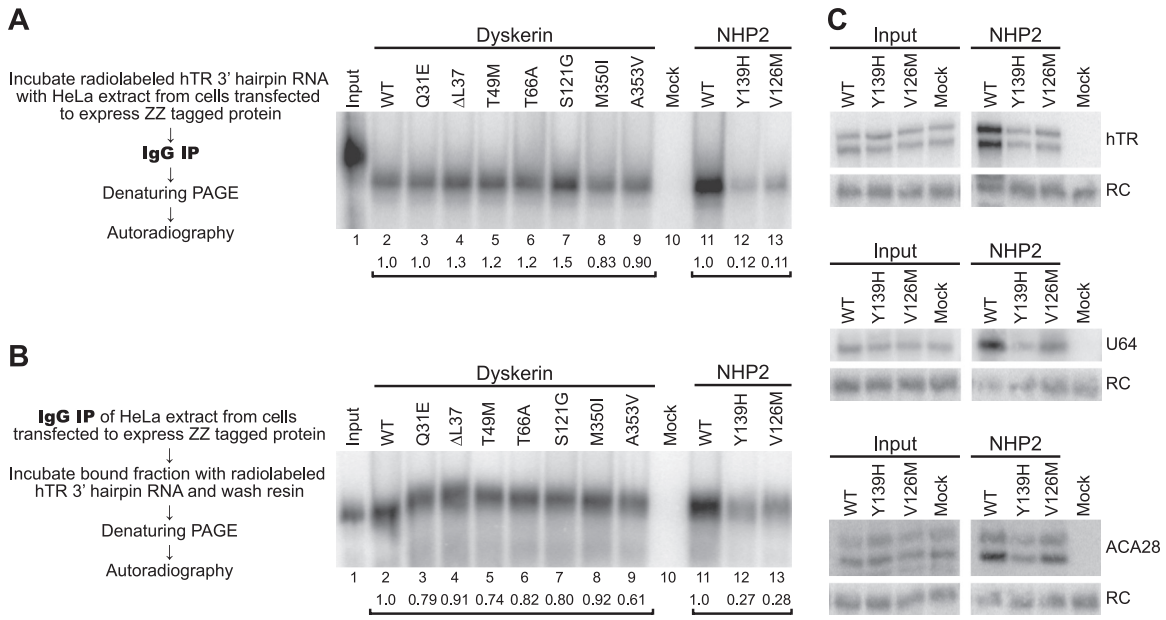

FIG 7 DC variants of NHP2 but not dyskerin inhibit hTR 3′ hairpin RNP assembly. (A) HeLa whole-cell extracts from cells transfected to express the indicated TAP-tagged dyskerin or ZZ-tagged NHP2 variant were incubated with radiolabeled PP7-tagged hTR 3′ hairpin RNA. Following RNP immunopurification and washing to remove unbound RNA, bound RNA (100%) was detected relative to input RNA (2%). Values below lane numbers are the normalized quantification of bound RNA within each bracketed set. (B) Complexes containing the tagged protein with the indicated variant sequence were immunopurified from whole-cell extract of transfected HeLa cells prior to incubation with radiolabeled PP7-tagged hTR 3′ hairpin RNA. Following washing to remove unbound RNA, bound RNA (100%) was detected relative to input RNA (2%). Values below lane numbers are the normalized quantification of bound RNA within each bracketed set. (C) Complexes containing tagged protein were immunopurified from whole-cell extracts of 293T cells transfected to express the indicated ZZ-tagged NHP2 variant and H/ACA RNA. RNPs were immunopurified by binding to and elution from IgG resin. A recombinant RNA recovery control (RC) was added to input cell extracts (2%) and purified RNPs (100%) prior to RNA extraction.

NHP2 variants are expressed heterozygously in DC patient cells, they would decrease but not eliminate functional NHP2. In sum, for the overexpressed disease-linked dyskerin and NHP2 variants tested here, we did not find an RNP assembly defect specific to hTR. Instead, we suggest that in their physiological genomic contexts, DC mutations impose phenotypes by reducing the cellular level of the preassembled RNA-binding-competent H/ACA core protein scaffold. This could result in a more dramatic reduction of mature hTR than other H/ACA RNAs, due to a differentially sensitized balance of precursor RNP assembly versus degradation.

DISCUSSION

Against our initial hypotheses for hTR BIO box function at an RNP biogenesis step that is not required for other human H/ACA RNAs, we found that the hTR BIO box influences a shared step of H/ACA RNP assembly. *In vivo* we suggest that hTR BIO box stimulation of RNP assembly tips the balance of hTR precursor protection versus exonucleolytic degradation. Degradation of a vertebrate telomerase RNA precursor may predominate over RNP assembly even in the presence of a BIO box, based on the increase in mature hTR accumulation resulting from insertion of a self-cleaving ribozyme that generates an exonuclease-resistant precursor 3′ end (Fig. 2D). Because intron-encoded H/ACA RNA precursors would be less sensitive to degradation within the host pre-mRNA transcript or within a spliced intron lariat, reducing the cellular level of the initial RNP assembly scaffold could preferentially compromise mature hTR accumulation without impact on other human H/ACA RNAs. Indeed, even hTR H/ACA domain accumulation becomes independent of BIO box function when the RNA is processed from intron context (41). We offer the unifying hypothesis that telomerase deficiency in DC patients with mutations that affect dyskerin, NOP10, or NHP2 results from reduced availability of the RNA-binding-competent H/ACA core protein scaffold. One prediction of this model is that the NAF1 promoter and/or open reading frame would be a locus of DC mutations.

Matching the two-hairpin specificity of eukaryotic H/ACA RNP assembly *in vivo*, we show that the resin-immobilized NAF1/dyskerin/NOP10/NHP2 scaffold has a two-hairpin requirement for binding pseudouridylation guide RNAs *in vitro*. Preorganization of two sets of core proteins as a NAF1-bound scaffold would account for the universality of the eukaryotic two-hairpin motif. *In vivo*, even if one of the two RNA hairpins is not biologically functional, its presence would still be required to give the second set of H/ACA proteins an RNA landing pad. This would account for why the biological accumulation of hTR depends on at least a minimal 5′ hairpin stem (13). The preorganized, NAF1-chaperoned H/ACA core protein scaffold may have been a eukaryotic adaption to increasing transcriptome complexity, which would have obliged enhanced discrimination of H/ACA RNP assembly on transcripts encoding advantageous modification guide RNAs versus the vast diversity of other transcription products.

From a structural perspective, it is notable that H/ACA RNA hairpins sharing the same consensus bind to the same protein scaffold with different affinities. This observation echoes previous findings of nonequivalence in protein recognition of a family of related nucleic acid binding sites (31). Like the hTR 3′ hairpin, the

single U17 3′ hairpin is sufficient to reconstitute as an H/ACA RNP *in vitro*. However, U17 does not share the specific sequence determinants that enhance hTR RNP assembly. U17 also does not substitute functionally for hTR H/ACA domain sequence *in vivo* (17). The features of the U17 3′ hairpin that enhance RNP assembly could act in a distributed manner, analogous to the assembly-enhancing sequence features of the hTR 3′ hairpin, or they could instead act by providing a U17-specific NAF1-RNA interaction (42).

From an evolutionary perspective, we note that although hTR and U17 gained 3′ hairpin features that enhance RNP assembly, other tested snoRNAs did not. The loss of pseudouridylation guide function by hTR and U17 may have provided the tolerance for a wider range of changes in hairpin structure. On the other hand, restrained from altering the architecture of RNA-protein interactions necessary for their function, vertebrate pseudouridylation guide RNAs instead gained an RNP assembly advantage by migrating into mRNA introns. Like the pseudouridylation guide H/ACA RNAs, U17 is intron encoded. For any known human H/ACA RNA other than hTR, there would be no detriment to expression in an intron context because 5′ and 3′ processing can generate the mature RNA independent of its flanking sequence. In contrast, hTR maturation is highly context dependent because 5′ processing would remove the functionally essential template. Therefore, as all other known vertebrate H/ACA RNAs migrated to genomic locations within mRNA introns, vertebrate telomerase RNAs had to remain independently transcribed genes. We suggest that this difference in the nascent RNA substrate for RNP assembly accounts for the preferential impact of disease-linked H/ACA protein variants on hTR accumulation *in vivo*.

ACKNOWLEDGMENTS

We thank Judy Wong for constructing the TAP-tagged dyskerin expression constructs.

This work was supported by NIH grant HL079585 to K.C.

REFERENCES

1. **Ballarino M, Morlando M, Pagano F, Fatica A, Bozzoni I.** 2005. The cotranscriptional assembly of snoRNPs controls the biosynthesis of H/ACA snoRNAs in *Saccharomyces cerevisiae*. Mol. Cell. Biol. **25**:5396–5403.
2. **Batista LF, et al.** 2011. Telomere shortening and loss of self-renewal in dyskeratosis congenita induced pluripotent stem cells. Nature **474**:399–402.
3. **Bird G, Fong N, Gatlin JC, Farabaugh S, Bentley DL.** 2005. Ribozyme cleavage reveals connections between mRNA release from the site of transcription and pre-mRNA processing. Mol. Cell **20**:747–758.
4. **Blackburn EH, Collins K.** 2010. Telomerase: an RNP enzyme synthesizes DNA, p 205–213. *In* Gesteland RF, Atkins JF, Cech TR (ed), RNA worlds, 4th ed. Cold Spring Harbor Laboratory Press, Cold Spring Harbor, NY.
5. **Cervelli M, et al.** 2002. Comparative structure analysis of vertebrate U17 small nucleolar RNA (snoRNA). J. Mol. Evol. **54**:166–179.
6. **Chao JA, Patskovsky Y, Almo SC, Singer RH.** 2008. Structural basis for the coevolution of a viral RNA-protein complex. Nat. Struct. Mol. Biol. **15**:103–105.
7. **Chen JL, Blasco MA, Greider CW.** 2000. Secondary structure of vertebrate telomerase RNA. Cell **100**:503–514.
8. **Darzacq X, et al.** 2006. Stepwise RNP assembly at the site of H/ACA RNA transcription in human cells. J. Cell Biol. **173**:207–218.
9. **Dennis PP, Omer A.** 2005. Small non-coding RNAs in Archaea. Curr. Opin. Microbiol. **8**:685–694.
10. **Dower K, Kuperwasser N, Merrikh H, Rosbash M.** 2004. A synthetic A tail rescues yeast nuclear accumulation of a ribozyme-terminated transcript. RNA. **10**:1888–1899.
11. **Dragon F, Pogacic V, Filipowicz W.** 2000. *In vitro* assembly of human H/ACA small nucleolar RNPs reveals unique features of U17 and telomerase RNAs. Mol. Cell. Biol. **20**:3037–3048.
12. **Duan J, Li L, Lu J, Wang W, Ye K.** 2009. Structural mechanism of substrate RNA recruitment in H/ACA RNA-guided pseudouridine synthase. Mol. Cell **34**:427–439.
13. **Egan ED, Collins K.** 2010. Specificity and stoichiometry of subunit interactions in the human telomerase holoenzyme assembled *in vivo*. Mol. Cell. Biol. **30**:2775–2786.
14. **Fatica A, Dlakic M, Tollervey D.** 2002. Naf1p is a box H/ACA snoRNP assembly factor. RNA **8**:1502–1514.
15. **Feng J, et al.** 1995. The RNA component of human telomerase. Science **269**:1236–1241.
16. **Fong N, Ohman M, Bentley DL.** 2009. Fast ribozyme cleavage releases transcripts from RNA polymerase II and aborts co-transcriptional pre-mRNA processing. Nat. Struct. Mol. Biol. **16**:916–922.
17. **Fu D, Collins K.** 2003. Distinct biogenesis pathways for human telomerase RNA and H/ACA small nucleolar RNAs. Mol. Cell **11**:1361–1372.
18. **Ganot P, Caizergues-Ferrer M, Kiss T.** 1997. The family of box ACA small nucleolar RNAs is defined by an evolutionarily conserved secondary structure and ubiquitous sequence elements essential for RNA accumulation. Genes Dev. **11**:941–956.
19. **Girard C, et al.** 2008. Characterization of a short isoform of human Tgs1 hypermethylase associating with small nucleolar ribonucleoprotein core proteins and produced by limited proteolytic processing. J. Biol. Chem. **283**:2060–2069.
20. **Hamma T, Ferre-D'Amare AR.** 2010. The box H/ACA ribonucleoprotein complex: interplay of RNA and protein structures in post-transcriptional RNA modification. J. Biol. Chem. **285**:805–809.
21. **Henras A, Dez C, Noaillac-Depeyre J, Henry Y, Caizergues-Ferrer M.** 2001. Accumulation of H/ACA snoRNPs depends on the integrity of the conserved central domain of the RNA-binding protein Nhp2p. Nucleic Acids Res. **29**:2733–2746.
22. **Hogg JR, Collins K.** 2007. RNA-based affinity purification reveals 7SK RNPs with distinct composition and regulation. RNA **13**:868–880.
23. **Jády BE, Bertrand E, Kiss T.** 2004. Human telomerase RNA and box H/ACA scaRNAs share a common Cajal body-specific localization signal. J. Cell Biol. **164**:647–652.
24. **Kiss T, Fayet-Lebaron E, Jady BE.** 2010. Box H/ACA small ribonucleoproteins. Mol. Cell **37**:597–606.
25. **Klein DJ, Schmeing TM, Moore PB, Steitz TA.** 2001. The kink-turn: a new RNA secondary structure motif. EMBO J. **20**:4214–4221.
26. **Koo BK, et al.** 2011. Structure of H/ACA RNP protein Nhp2p reveals cis/trans isomerization of a conserved proline at the RNA and Nop10 binding interface. J. Mol. Biol. **411**:927–942.
27. **Li H.** 2008. Unveiling substrate RNA binding to H/ACA RNPs: one side fits all. Curr. Opin. Struct. Biol. **18**:78–85.
28. **Li S, Duan J, Li D, Ma S, Ye K.** 2011. Structure of the Shq1-Cbf5-Nop10-Gar1 complex and implications for H/ACA RNP biogenesis and dyskeratosis congenita. EMBO J. **30**:5010–5020.
29. **Li S, et al.** 2011. Reconstitution and structural analysis of the yeast box H/ACA RNA-guided pseudouridine synthase. Genes Dev. **25**:2409–2421.
30. **Liang B, et al.** 2009. Structure of a functional ribonucleoprotein pseudouridine synthase bound to a substrate RNA. Nat. Struct. Mol. Biol. **16**:740–746.
31. **Meijsing SH, et al.** 2009. DNA binding site sequence directs glucocorticoid receptor structure and activity. Science **324**:407–410.
32. **Mitchell JR, Cheng J, Collins K.** 1999. A box H/ACA small nucleolar RNA-like domain at the human telomerase RNA 3′ end. Mol. Cell. Biol. **19**:567–576.
33. **Mitchell JR, Collins K.** 2000. Human telomerase activation requires two independent interactions between telomerase RNA and telomerase reverse transcriptase *in vivo* and *in vitro*. Mol. Cell **6**:361–371.
34. **Mitchell JR, Wood E, Collins K.** 1999. A telomerase component is defective in the human disease dyskeratosis congenita. Nature **402**:551–555.
35. 12/$12.00 Molecular and Cellular Biology p. 2428–2439**Nolivos S, Carpousis AJ, Clouet-d'Orval B.** 2005. The K-loop, a general feature of the *Pyrococcus* C/D guide RNAs, is an RNA structural motif related to the K-turn. Nucleic Acids Res. **33**:6507–6514.

36. **O'Sullivan RJ, Karlseder J.** 2010. Telomeres: protecting chromosomes against genome instability. Nat. Rev. Mol. Cell Biol. **11**:171–181.
37. **Podlevsky JD, Bley CJ, Omana RV, Qi X, Chen JJ.** 2008. The telomerase database. Nucleic Acids Res. **36**:D339–D343.
38. **Richard P, Kiss AM, Darzacq X, Kiss T.** 2006. Cotranscriptional recognition of human intronic box H/ACA snoRNAs occurs in a splicing-independent manner. Mol. Cell. Biol. **26**:2540–2549.
39. **Shay JW, Wright WE.** 2010. Telomeres and telomerase in normal and cancer stem cells. FEBS Lett. **584**:3819–3825.
40. **Steinmetz EJ, Conrad NK, Brow DA, Corden JL.** 2001. RNA-binding protein Nrd1 directs poly(A)-independent 3′-end formation of RNA polymerase II transcripts. Nature **413**:327–331.
41. **Theimer CA, Jády et al.** 2007. Structural and functional characterization of human telomerase RNA processing and Cajal body localization signals. Mol. Cell **27**:869–881.
42. **Trahan C, Dragon F.** 2009. Dyskeratosis congenita mutations in the H/ACA domain of human telomerase RNA affect its assembly into a pre-RNP. RNA **15**:235–243.
43. **Trahan C, Martel C, Dragon F.** 2010. Effects of dyskeratosis congenita mutations in dyskerin, NHP2 and NOP10 on assembly of H/ACA pre-RNPs. Hum. Mol. Genet. **19**:825–836.
44. **Vulliamy T, et al.** 2001. The RNA component of telomerase is mutated in autosomal dominant dyskeratosis congenita. Nature **413**:432–435.
45. **Wang C, Meier UT.** 2004. Architecture and assembly of mammalian H/ACA small nucleolar and telomerase ribonucleoproteins. EMBO J. **23**:1857–1867.
46. **Wong JMY, Collins K.** 2006. Telomerase RNA level limits telomere maintenance in X-linked dyskeratosis congenita. Genes Dev. **20**:2848–2858.
47. **Xiao M, Yang C, Schattner P, Yu YT.** 2009. Functionality and substrate specificity of human box H/ACA guide RNAs. RNA **15**:176–186.
48. **Yang PK, et al.** 2005. Cotranscriptional recruitment of the pseudouridylsynthetase Cbf5p and of the RNA binding protein Naf1p during H/ACA snoRNP assembly. Mol. Cell. Biol. **25**:3295–3304.
49. **Zhang Q, Kim NK, Feigon J.** 2011. Architecture of human telomerase RNA. Proc. Natl. Acad. Sci. U. S. A. **108**:20325–20332.